

First DØ Jet Measurements at $\sqrt{s} = 1.96$ TeV

D. Lincoln^a (for the DØ Collaboration)

^aFermi National Accelerator Laboratory, Box 500, Batavia, IL 60510 USA

We present the first QCD measurements performed by the DØ experiment for Fermilab's Run II. These measurements are the inclusive jet p_T and di-jet mass cross-sections. These analyses were performed using an integrated luminosity of 34 pb^{-1} . Included also are comparisons to next-to-leading order QCD predictions from the JETRAD program. Within experimental uncertainties, data and theory are in good agreement.

The DØ experiment is a large multi-purpose particle detector, located at the Fermilab Tevatron. Commencing operations in 1992, the detector collected data with an approximate integrated luminosity of 100 pb^{-1} before its shutdown in 1996. This data yielded over 100 publications on a vast range of research topics, most notably the co-discovery of the top quark in 1995. This data collection period is called Run I.

During the intervening years, the DØ experiment has undertaken an aggressive upgrade so as to be able to exploit a corresponding upgrade of the Fermilab accelerator complex. Fermilab's accelerator improvements will increase the center of mass collision energy to 1.96 TeV, a 9% increase over its original collision energy of 1.8 TeV, yielding as much as a factor of 5 increase in cross-section at the highest energies (see figure 1). In addition, a factor of 20 increase in integrated luminosity to a full 2 fb^{-1} is anticipated, with an additional increase to 30 fb^{-1} possible prior to the turn on of the LHC.

The DØ detector's upgrade has left it with a central tracker consisting of a silicon microstrip detector, comprising 800,000 channels, surrounded by an innovative tracker consisting of scintillating fiber, read out by Visible Light Photon Counters (VLPCs) [1]. The entire tracker sits in a solenoidal magnetic field of strength 2 Tesla. Particles' energies are measured by a uranium/liquid argon calorimeter, unchanged from Run I, although with new electronics necessary to cope with the Tevatron's increased luminosity and reduced crossing time. Surrounding the

calorimeter is a muon detector consisting of three planes of scintillator and drift-tubes, sandwiching a toroidal magnet. In addition, DØ's upgrade includes the forward proton detector, a series of Roman Pots integrated into the Tevatron lattice to explore diffractive physics.

Since recommencing operations in March 2001, DØ has recorded 126 pb^{-1} of integrated luminosity, although the data presented here only utilizes 34 pb^{-1} in order to ensure that only the best quality data is presented.

The most common sorts of physics processes observed at the Tevatron are jet production, the measurement of which can shed light on the nature of the strong force, constrain the parton distribution functions and search for new physics [2]. In DØ, jets are reconstructed using a standard iterative cone algorithm, with $R = 0.7$ ($R^2 = \Delta\eta^2 + \Delta\phi^2$). The jet energy as measured in the DØ calorimeter is corrected back to the particle level by using photon-jet events which utilize the fact that the photon energy is measured very well and conservation of transverse momentum which constrains the jet p_T . There are statistical and systematic uncertainties associated with the jet energy correction, which increases as a function of jet p_T . The increase is mostly due to extrapolation as the photon-jet event statistics run out at about 200 GeV. Continued data-taking will eventually extend this range. In order to reduce measurement uncertainty caused by this temporary uncertainty in jet energy correction, we restrict our analysis to jets with pseudorapidity $|\eta| < 0.5$, which is the region of the detector in which the

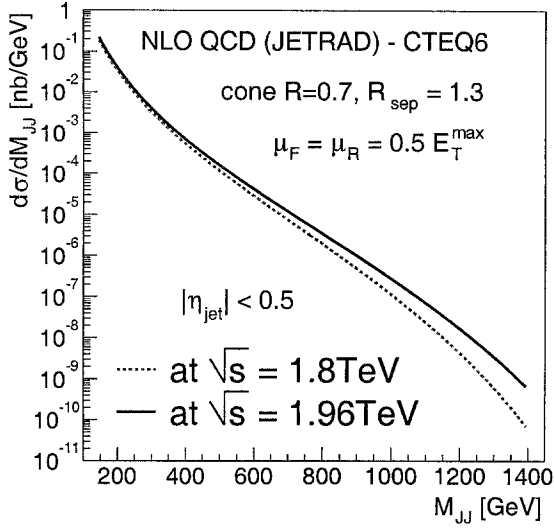


Figure 1. Predicted theoretical dijet mass cross-sections for both a collision energy of 1.96 and 1.8 TeV. At higher masses, the increase in cross-section can reach a factor of 5.

correction and associated uncertainties are best understood.

In this proceedings, we present two measurements; the inclusive jet p_T and dijet-mass cross sections. Data was taken using DØ's three-level trigger system, which is similar to that reported in [3]. DØ's highest level jet trigger is constructed by using a non-iterative η - ϕ cone and requiring a minimum p_T in the cone. Due to the strong drop in jet cross-section as a function of jet p_T , a total of 5 triggers were implemented, with lower p_T triggers prescaled by a progressively larger factor, so as to not saturate the data acquisition bandwidth. These triggers had a minimum p_T of 25, 45, 65 and 95 GeV, with an additional trigger requiring only a minimal amount of energy in the calorimeter, so as to be able to characterize the turn on of the 25 GeV trigger.

Figure 2 shows the uncorrected inclusive jet cross-section, where the data for each trigger is normalized to its respective luminosity and

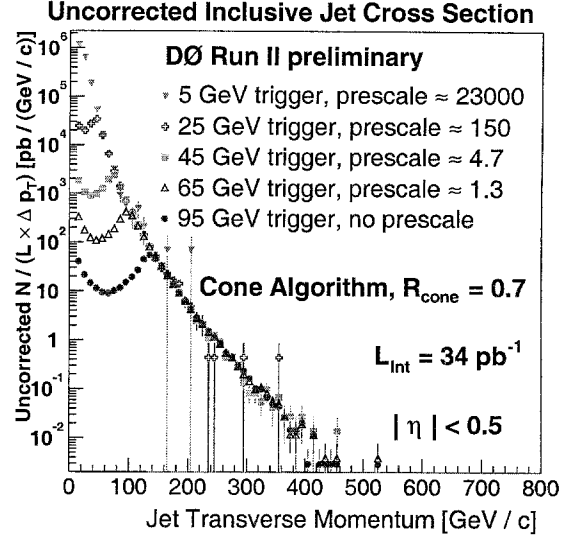


Figure 2. Trigger turn-on for the inclusive jet p_T cross-section.

prescale factor. This figure shows that each of the low p_T triggers supplies approximately 3 bins to the overall cross-section, while the highest p_T trigger supplies many more. Figure 3 shows a similar result for the dijet mass cross-section.

The dijet mass sample is a subset of the inclusive jet p_T distribution sample, comprising those events where both of the two highest p_T jets were central (i.e. $|\eta| < 0.5$). The p_T resolution of the jets was determined by evaluating the p_T imbalance between the two leading jets in the limit where the transverse momentum of the third jet approaches zero. This resolution was used to determine the unsmearing correction for the inclusive jet p_T distribution (10 – 15%) and the dijet mass spectrum (5 – 15%). The correction function was determined from a theoretically-motivated ansatz function which, when smeared by the experimentally determined jet resolution, corresponds to the uncorrected data. The ratio of the unsmearing over the smeared ansatz function gives the correction.

Figure 4 shows the fully corrected inclusive jet

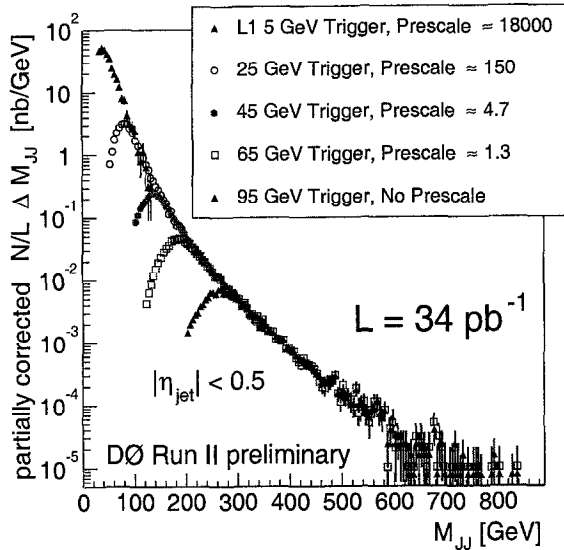


Figure 3. Trigger turn-on for the dijet mass cross-section.

p_T cross-section, while figure 5 shows the dijet mass cross-section. Overlaid on both is a perturbative QCD theoretical prediction as supplied by JETRAD [4], using the specific choice of the CTEQ6M [5] parton distribution function. The factorization and normalization scales are both set to $p_T/2$. In addition, the R_{SEP} parameter (related to the minimum separation in $\eta-\phi$ space between two jets in units of cone size) is 1.3. Varying factorization and normalization scales and R_{SEP} parameter by reasonable values affects the cross-section predictions by about 10%.

Figures 6 and 7 show linearized versions of figure 4, while figures 8 and 9 show linearized versions of figure 5. Again, we use JETRAD and the CTEQ6M parton distribution functions as well as another modern PDF from the MRST group (MRST2001 [6]). In these plots, the statistical and systematic uncertainties (removing luminosity and energy scale ambiguities) are attached to each data point, while the uncertainty due to energy scale is denoted by the large bands. The uncertainty due to the jet energy scale correction

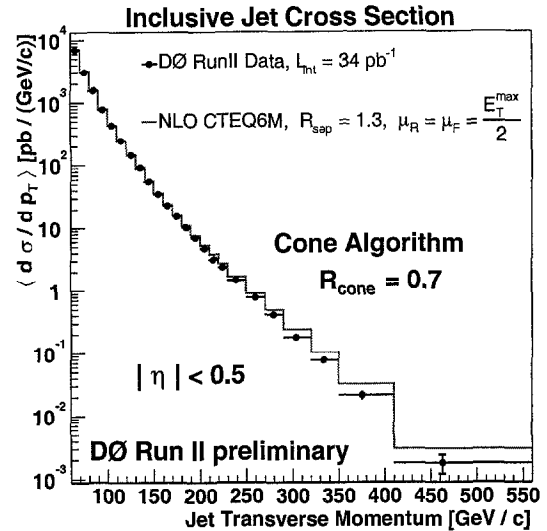


Figure 4. Corrected inclusive jet p_T cross-section (preliminary).

dominates, ranging from 50% at the lowest energy bins, to approximately 100% at the highest energies. While the error bars are sufficiently large so as to preclude discriminating between the two parton distribution functions, their slightly different shapes and normalization are of theoretical interest.

In this proceedings, we have presented DØ's first jet production results from Run II, measuring high p_T jet phenomena. Data taking is ongoing and with the increased dataset, a decrease in the jet energy calibration uncertainties is expected as well as increased statistics in the highest p_T and dijet mass bins.

REFERENCES

1. A. Bross *et al.*, "Characterization and Performance of Visible Light Photon Counters (VLPCs) for the Upgraded DØ Detector at the Fermilab Tevatron," Nucl. Instrum. and Meth. **A477** 172 (2002).
2. D. Stump *et al.*, "Inclusive jet production,

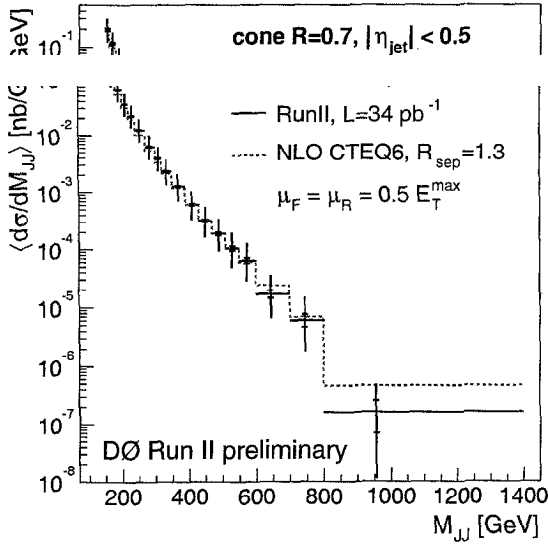


Figure 5. Corrected dijet mass cross-section (preliminary).

- parton distributions and the search for new physics," hep-ph/0303013.
3. G.C. Blazey (for the DØ Collaboration), "The DØ Run II Trigger", FERMILAB-CONF-97-395-E.
 4. W. T. Giele, E.W. Glover and D. A. Kosower, "Higher Order Corrections to Jet Cross-Sections in Hadron Colliders," Nucl. Phys. B403 633 (1993).
 5. J. Pumplin *et al.*, "New Generation of Parton Distributions with Uncertainties from a Global QCD Analysis", JHEP 0207 012 (2002).
 6. A.D. Martin *et al.*, "MRST2001: Partons and α_s from Precise Deep Inelastic Scattering and Tevatron Jet data," Eur. Phys. J C23, 73 (2002).

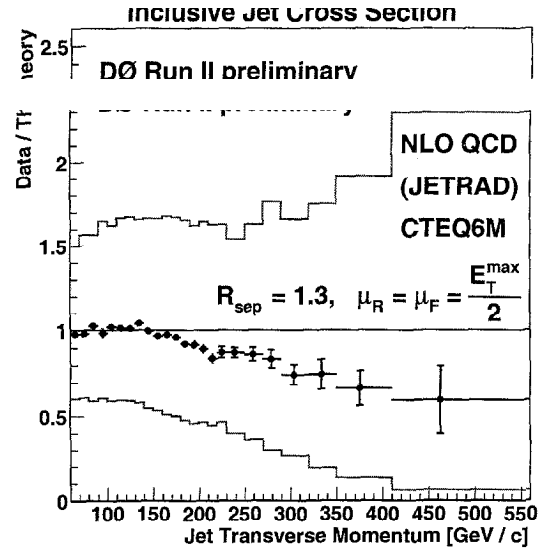


Figure 6. Linearized comparison of inclusive jet p_T cross-section to JETRAD calculation, using the CTEQ6M pdf (preliminary).

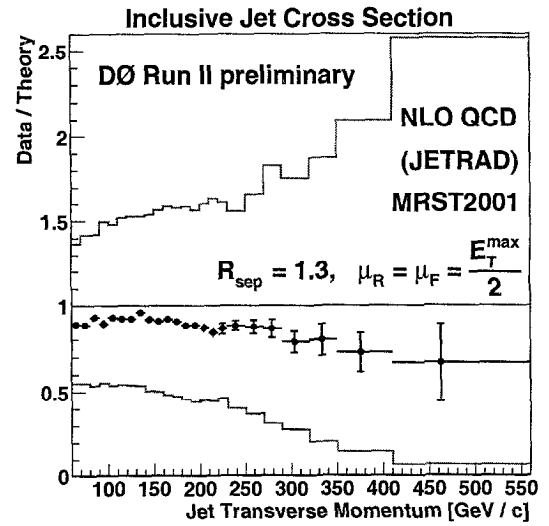


Figure 7. Linearized comparison of inclusive jet p_T cross-section to JETRAD calculation, using the MRST2001 pdf (preliminary).

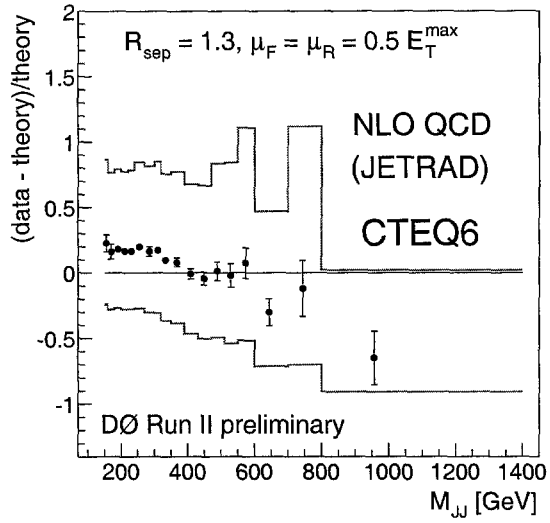


Figure 8. Linearized comparison of the dijet mass cross-section to JETRAD calculation, using the CTEQ6M pdf (preliminary).

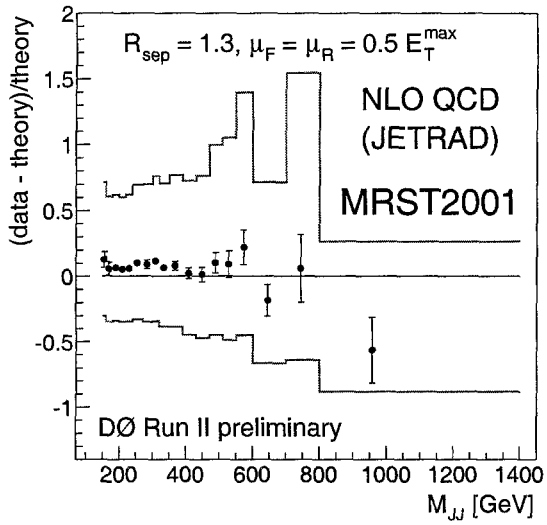


Figure 9. Linearized comparison of the dijet mass cross-section to JETRAD calculation, using the MRST2001 pdf (preliminary).